DEPARTMENT OF CHEMISTRY
RADIOCHEMISTRY
UNIVERSITY OF HELSINKI

Neptunium(V) interactions with the bentonite clay barrier constituents bentonite, montmorillonite, corundum and granitic host rock

Licentiate Thesis

Outi Hanna Maria Elo

22.9.2019

HELSINGIN YLIOPISTO
HELSINGFORS UNIVERSITET
UNIVERSITY OF HELSINKI

Tiedekunta – Fakultet – Faculty Faculty of Science		Koulutusohjelma – Utbildningsprogram – Degree Programme Doctoral Programme in Chemistry and Molecular Sciences (CHEMS)
Opintosuunta – Studieinriktning – Study Track Molecular Science, Radiochemistry		
Tekijä – Författare – Author Outi Hanna Maria Elo		
Työn nimi – Arbetets titel – Title Neptunium(V) interactions with the bentonite clay barrier constituents bentonite, montmorillonite, corundum and granitic host rock		
Työn laji – Arbetets art – Level Licentiate Thesis	Aika – Datum – Month and year 09 / 2019	Sivumäärä– Sidoantal – Number of pages 44

Tiivistelmä – Referat – Abstract

The scope of this thesis was to investigate the uptake of the actinide neptunium-237 (^{237}Np) by solid phases of relevance for the disposal of spent nuclear fuel (SNF) in deep, granitic underground repositories. Investigations were performed with the mineral phases corundum (α-Al_2O_3) and montmorillonite ($(Na)_{0.33}(Al,Mg)_2(Si_4O_{10})(OH)_2 \cdot nH_2O$) as well as with bentonite colloids and crushed Kuru gray granite, which are constituents of the Engineered Barrier System (EBS), and the host-rock, respectively.

The uptake of neptunium in the pentavalent oxidation state (NpO_2^+) by these solid phases was investigated by batch sorption experiments, which provided information about the quantity of neptunium(V) removal from solution as a function of pH, neptunium concentration, and mineral concentration. By repeated exchange of the background electrolyte it was possible to obtain information about the desorption of neptunium(V) from the mineral surfaces, and to gain an insight into the potential re-mobilization of the actinide under flowing-water conditions.

As batch sorption and desorption experiments do not provide information about the exact chemical species of neptunium on the mineral surface, the macroscopic sorption experiments were complemented by spectroscopic investigations using Attenuated Fourier Transform Infra-red (ATR FT-IR) and Extended X-ray Absorption Fine Structure (EXAFS) spectroscopies. This enabled the extraction of the complex structure and speciation of neptunium on the solid surfaces including bond lengths, neighboring atoms, coordination numbers and the type of surface complex formed on the solid phases, i.e. outer- vs. inner-sphere bound neptunium.

Most of the investigations were performed under stagnant conditions, however, due to the role of potential stable and mobile colloids in the subsurface environment and their role as carriers and mobilizers of colloid-borne neptunium with flowing groundwater, additional granite column experiments were conducted in the absence and presence of bentonite colloids. Here, the migration of neptunium through the column was investigated as a function of time, and the role of colloids was evaluated from the obtained breakthrough curves. Under the chosen experimental conditions, colloids were found to have a negligible influence on the neptunium(V) breakthrough behavior, where most of the neptunium(V) was found to migrate through the column without adsorption onto the granitic column material.

Avainsanat – Nyckelord – Keywords
Neptunium(V), Sorption, Montmorillonite, Corundum, Surface complexation, X-ray absorption spectroscopy, ATR FT-IR spectroscopy, Bentonite colloids, Granitic rock, Column experiments

Säilytyspaikka – Förvaringställe – Where deposited
E-thesis

Muita tietoja – Övriga uppgifter – Additional information

CONTENTS

1 LIST OF PUBLICATIONS

This licentiate thesis is based on the following original publications, which are referred to in the text by their Roman numerals (I – II).

I. O. Elo, K. Müeller, A. Ikeda-Ohno, F. Bok, A.C. Scheinost, P. Hölttä and N. Huittinen (2017) Batch sorption and spectroscopic speciation studies of neptunium uptake by montmorillonite and corundum, Geochimica et Cosmochimica Acta, *198*, 168 – 181.

II. O. Elo, P. Hölttä, P. Kekäläinen, M. Voutilainen and N. Huittinen (2019) Neptunium(V) transport in granitic rock: A laboratory scale study on the influence of bentonite colloids, Applied Geochemistry, *103*, 31 – 39.

Author's contributions to the publications:

In Papers I and II the author performed the majority of the experiments, the data analysis and interpretation. In paper I, ATR FT-IR and EXAFS measurements and data analysis were performed together with the coauthors, while surface complexation modeling was performed fully by one of the coauthors. In paper II, the modeling of column breakthrough curves was performed by coauthors. The author has planned and written the manuscripts with input from all coauthors.

List of abbreviations

ATR FT-IR	Attenuated Total Reflection Fourier Transform Infra-Red
DLS	Dynamic Light Scattering
DDL	Diffuse Double-Layer
EBS	Engineered Barrier System
ESRF	European Synchrotron Radiation Facility
EXAFS	Extended X-ray Absorption Fine Structure
ICP-MS	Inductively Coupled Plasma Mass Spectrometry
K_d	Sorption distribution coefficient
LSC	Liquid Scintillation Counting
ROBL	Rossendorf Beamline
SNF	Spent Nuclear Fuel
PCS	Photon Correlation Spectroscopy
XANES	X-ray Absorption Near-Edge structure
XRD	X-Ray Diffraction

1 INTRODUCTION

1.1 Neptunium-237

The radioactive actinide neptunium-237 is one of the major dose contributors in Spent Nuclear Fuel (SNF) after one hundred thousand years due to its long half-life of 2.144×10^6 years (Hursthouse et al., 1991; Kaszuba and Runde, 1999; Zhao et al., 2014). Neptunium-237 is produced directly from uranium (U-235 and U-238) by neutron activation and subsequent beta decay. Under natural conditions, neptunium exists in mainly two oxidations states, IV and V, of which the first is dominating under anoxic, mildly reducing conditions and the latter one under oxic conditions. In the tetravalent oxidation state neptunium hydrolyzes easily, is readily adsorbed on solid surfaces, and can form solid NpO_2 depending on the prevailing environmental conditions, thus, making the actinide rather immobile. In mildly oxic groundwater conditions pentavalent neptunium is present as the neptunyl cation NpO_2^+ which is soluble, poorly sorbed by solid surfaces, and therefore easily migrates with the groundwater (Viswanathan et al., 1998; Kaszuba and Runde, 1999; Kozai et al., 2014). Therefore, the focus of this thesis was on the migration behavior of neptunium(V) in the presence of solid phases of relevance for the disposal of SNF, as described in the following chapters.

1.2 Engineered barrier system for spent nuclear fuel disposal

The engineered barrier system for the disposal of spent nuclear fuel in Finland consists of copper canisters with cast iron inserts, buffer material between the canister and the granitic bedrock, tunnel backfill material, and the bedrock itself (Hellä et al., 2014). The ceramic uranium pellets in the Zircaloy-coated fuel rods are packed in the copper canisters which provide corrosion protection for at least some hundred thousands of years. The cast iron insert provides mechanical protection against earthquakes and the pressure caused by the ice cap during the next glacial-interglacial period (Pastina and Hellä, 2006). The buffer between the canister and bedrock protects the canisters from earthquakes, limits water intrusion into the near-field of the waste canisters, and limits release of radionuclides if the canister fails. The tunnel backfill increases the stability of the tunnels and provides predictable mechanical, geochemical, and hydrogeological conditions for the canisters. The final

barrier is the bedrock itself which in Finland belongs to the Northern and Eastern Europe's tectonically stable Fennosarmatian craton. The bedrock is mainly granite (53%) and migmatic rocks (22%). The migmatic gneiss makes the bedrock stable and protects the canisters from groundwater (Vieno and Nordman, 1999). The bedrock isolates the repository from the surface environment and approximately two meters of solid rock suppresses the radiation dose from the SNF to the level of natural background. (Hellä et al., 2014).

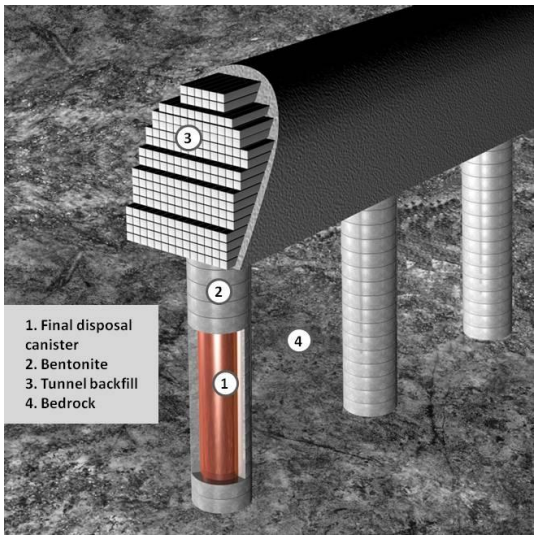

Figure 1. Multi-barrier principle showing how the canisters will be set in the deep geological repository with bentonite. (Posiva Oy)

In the following thesis, the role of the buffer barrier on the immobilization of neptunium(V) was investigated in detail. For this purpose, the buffer material bentonite was chosen for the studies, as it is considered as a buffer in several SNF repository concepts e.g. in Scandinavia, Switzerland, and France due to its low hydraulic conductivity, swelling ability and high specific surface area, which is prone to sorb radionuclides released from the SNF (Missana et al., 2003; 2011). The drawback of the bentonite buffer is its tendency to form mobile and stable colloids below the so called Critical Coagulation Concentration (CCC) (Lagaly and Ziesmer, 2003; Tombácz and Szekeres, 2004; García-García et al., 2007). Such environmental conditions in the EBS could be reached due to dilution of groundwater after a possible glacial period. Thus, studies involving bentonite colloids in granitic environments,

simulating the potential migration of neptunium(V) with mobile colloids were included in this thesis.

Bentonite consists of several mineral phases such as montmorillonite, muscovite, quartz, plagioclase, illite, tridymite, magnetite, gypsum and pyrite. The main constituent, however, is the mineral montmorillonite ($(Na)_{0.33}(Al,Mg)_2(Si_4O_{10})(OH)_2 \cdot nH_2O$) which is a TOT-structured clay mineral. TOT refers to the different layers in montmorillonite, consisting of tetrahedral (T) Si(IV) units and octahedral (O) Al(III) units, see Figure 2. The cations in the different layers undergo ion replacement (e.g. Si^{4+} is replaced by Al^{3+}) causing a permanent negative charge of the clay mineral. In addition, silanol and aluminol groups at the edge sites are responsible for so called pH-dependent charge, through protonation and deprotonation reactions of the surface hydroxyl groups depending on the surrounding pH.

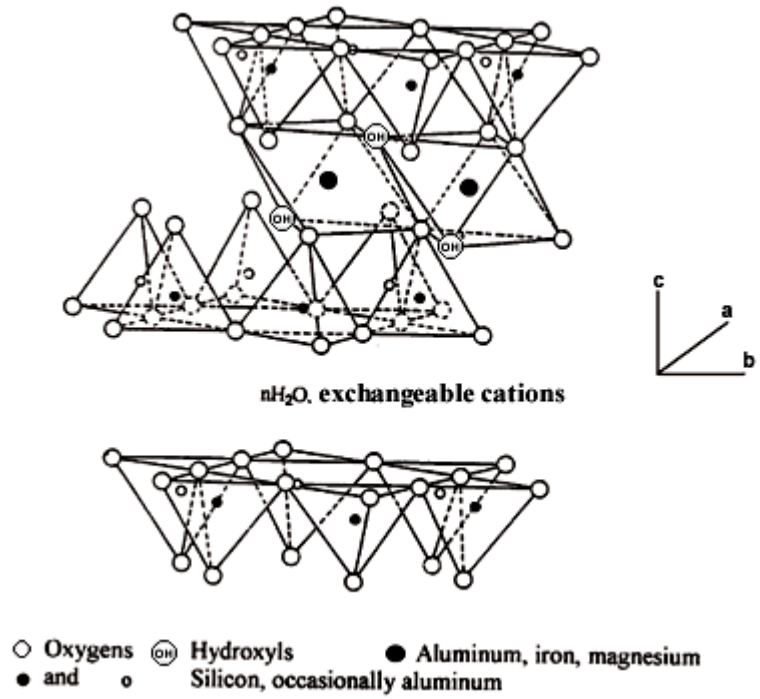

Figure 2. Typical two layer structure for smectites. For montmorillonite the black dots stand for aluminum (Grim 1968).

Due to the relevance of montmorillonite in the bentonite buffer, both solid phases were chosen for this thesis as representatives for the buffer barrier in a final

repository for SNF. In addition, the aluminum oxide corundum (α-Al_2O_3) was used in parallel in some of the studies, to represent the aluminol groups on the montmorillonite surface. Actinide retention onto these solid components will be discussed in the following chapter.

1.3 Sorption of actinides on EBS components

1.3.1 Sorption mechanisms

Released actinides from the SNF may retain on the buffer material through various sorption mechanisms such as inner-sphere and outer-sphere complexation. In inner-sphere complexation, a chemical bond is formed between the actinide and the surface oxygen atom(s). In outer-sphere complexation the positively charged actinide cation is being attracted to the negatively charged functional surface groups through electrostatic interactions. Cations that adsorb by outer-sphere complexation and are readily exchangeable with similar ions in solution, i.e. changes in the ionic strength may strongly influence the extent of outer-sphere sorption. The capacity of a mineral to retain a cation by ion exchange can be described with the Cation Exchange Capacity (CEC).

Montmorillonite is known to readily retain radionuclides by cation exchange in the interlayer space (Birgersson and Karnland, 2009; Hartmann et al., 2011), or through surface complexation of the functional surface groups on the mineral edges (Bradbury and Baeyens, 2002; Sabodina et al., 2006; Zavarin et al., 2012). Radionuclide sorption on montmorillonite has been investigated in several studies (Marques Fernandes et al., 2012; Missana et al., 2014; Soltermann et al., 2014). However, only few studies investigating neptunium(V) uptake by montmorillonite can be found (Turner et al., 1998; Nagasaki and Tanaka, 2000; Bradbury and Baeyens, 2006; Sabodina et al., 2006; Zavarin et al., 2012; Kozai et al., 2014).

The double layer structure of montmorillonite allows formation of both outer- and inner-sphere complexes. Corundum (α-Al_2O_3) consists of hexagonal close packed layers of AlO_6 octahedra, the hydroxyl groups deprotonate under alkaline conditions where formation of inner-sphere complex is possible. Since corundum does not have permanent surface charge and it has a rather high isoelectric point (IEP) where the

net surface charge is zero, it does not form outer-sphere complexes (Kupcik et al., 2016).

The bentonite buffer has been shown to have a strong sorption capacity for radionuclides in the tri- and tetravalent oxidation states (Zhao et al., 2008; Huber et al., 2011; Verma et al., 2014; Begg et al., 2015). Hexavalent uranyl(VI) uptake by bentonite has been shown to be dependent of the bentonite material and the environmental conditions (Missana et al., 2004; Bachmaf et al., 2008; Ren et al., 2010; Huber et al., 2011; Zong et al., 2015). Only few studies have been investigating the uptake of pentavalent radionuclides by bentonite, however, existing experiments have shown an increased uptake of neptunium(V) and plutonium(V) under alkaline conditions (Begg et al., 2015; Li et al., 2015; Sabodina et al., 2016).

1.3.2 Batch sorption studies

Batch sorption experiments are the simplest way to investigate the removal of an actinide from solution, through attachment on a solid surface. In its simplest form, sorption is described by the sorption percentage according to equation 1.

$$Sorption\ \% = \frac{c_0 - c_{measured}}{c_0} \quad (1)$$

where c_0 is the initial actinide concentration and $c_{measured}$ the actinide concentration in supernatant at the end of sorption experiment.

The sorption percentage cannot be used to compare different sorbents, as the percentage is dependent on several parameters, such as the concentration of the actinide, the amount and the specific surface area of the solid phase. To account for the latter parameters, sorption distribution coefficients (K_d) are used to describe the sorption reaction, equation 2.

$$K_d\left(\frac{ml}{g}\right) = \frac{equilibrium\ mass\ of\ actinide\ sorbed\ on\ solid}{equilibrium\ mass\ of\ actinide\ in\ solution} * \left(\frac{V}{m}\right) \quad (2)$$

where V is the volume of the solution and m is the mass of the solid phase.

Thus, K_d describes the ratio between sorbed and non-sorbed cations in suspension. If the K_d-values are normalized with respect to the specific surface area of the sorbent, the distribution coefficient can be used to compare sorption capacities of different minerals and compounds.

Finally, to account for concentration effects on the sorption reactions, adsorption isotherms, which describe the ratio between sorbed and non-sorbed actinide in the suspension as a function of actinide concentration, are used. Adsorption isotherms are plotted as the amount of sorbed species (mol/kg) against the amount of non-sorbed species (mol/l). A slope of one for a sorption isotherm indicates that sorption is constant or ideal, whereas a slope below one speaks for surface site saturation, steric effects, or the presence of different types of sorption sites with differing complexation strength. In literature, these sites are referred to as strong and weak sites, where the former ones are less abundant and dominate the metal ion uptake at low actinide concentrations, while the latter site type is much more abundant and participates in the sorption reaction at higher overall actinide concentrations.

In the present work neptunium(V) uptake by montmorillonite, corundum, bentonite colloids and Kuru gray granite were investigated as a function of pH in batch type experiments. The nature of the sorption sites (strong v.s weak sites) and possible saturation of the sorption sites were investigated as a function of neptunium concentration. These isotherm investigations were conducted for montmorillonite, corundum, and bentonite colloids. The effect of the solid concentration and sorption kinetics on the uptake of neptunium was investigated for montmorillonite. These experiments give valuable information about the optimum experimental conditions maximizing the amount of neptunium(V) sorption on the mineral surface. Batch sorption studies are typically performed under stagnant conditions. Therefore, conclusions about the neptunium(V) uptake behavior under flowing water conditions, which could exist after water ingress into the SNF repository, cannot be drawn. To investigate the influence of flowing water conditions, desorption experiments, where the background electrolyte was exchanged to a fresh one every 2 to 3 days were performed to observe the reversibility of neptunium(V) uptake by montmorillonite and corundum. In addition to the desorption experiments, column

experiments were conducted. These experiments simulate the behavior of neptunium(V) in groundwater, where neptunium(V) can exist as mobile neptunyl cation and retain on the granitic bedrock or sorb on mobile bentonite colloids. Neptunium(V) retardation on granitic rock can be investigated in column experiments using a conservative tracer as reference, which elutes through the column without interfering with granitic rock. Influence of bentonite colloids on neptunium(V) migration was studied in the presence and absence of bentonite colloids to deduce whether the presence of bentonite colloids would enhance neptunium(V) migration through the column or not.

1.3.3 Spectroscopic speciation studies

Batch sorption experiments do not provide information about the exact chemical species of neptunium on the mineral surface. Therefore, spectroscopic methods have to be used, which are capable of probing the direct actinide environment either on the solid phase or in suspension. In the present thesis, two independent spectroscopic methods, Attenuated Total Reflection Fourier Transform Infra-Red (ATR FT-IR) and Extended X-ray Absorption Fine Structure (EXAFS), were used to study the neptunium(V) sorption reaction on the chosen solid phases.

ATR FT-IR spectroscopy can be used to determine sorption complexes in solid-water surfaces based on characteristic vibrational modes (Müller et al., 2012). In comparison to other spectroscopic methods, ATR FT-IR spectroscopy gives the opportunity to monitor the solid-water interface *in situ*, instead of freezing and exposing samples under vacuum when there is a risk that the nature of a chemical bond could change (Lefevre, 2004). ATR FT-IR spectroscopy provides information about reactions at the interface between a solid surface and the aqueous phase at a molecular level. Based on the stretch vibration frequency of the An=O bond, conclusions can be drawn whether the formed chemical bond is coordinated inner spherically with surface sites or whether it is less specifically adsorbed by electrostatic or hydrophobic attractions to the surface (Hug and Sulzberger, 1994). Since inner-sphere complex formation includes a change in the actinide coordination, a change in position of the absorption band can be seen. For outer-sphere complexes only a small change of the absorption band position in comparison to the aquo ion is

expected. The method is based on reaction induced difference spectroscopy where a single beam IR spectrum of the stationary phase (in this study the mineral film) is continuously recorded while being rinsed with an eluent. First, the stationary phase is flushed with a blank solution in order to equilibrate the mineral film and ensure its stability. After that, the mineral film is being flushed with eluent containing sorbing cations or anions. Since the spectrum of the mineral film is being recorded with an acquisition time of 30 s, ATR FT-IR spectroscopy enables the monitoring of the sorption process with a time resolution of less than a minute. As cations adsorb on the mineral surface, the following adsorption changes can be observed in the difference spectrum of the mineral film before and after cation introduction. During the final step of the measurement, the mineral film is flushed again with the blank solution, which gives information about the reversibility of the sorption process (Müller et al. 2012). Neptunium(V) sorption on other mineral oxide surfaces such as TiO_2, $Al(OH)_3$ and Fe_2O_3 has been investigated in previous studies (Müller et al., 2009, 2015; Gückel et al., 2013) using ATR FT-IR spectroscopy, these results indicated formation of an inner-sphere complex on these mineral surfaces.

EXAFS is based on x-ray absorption by the actinide and, thus, the resulting absorption spectra are unique to each element due to different electron binding energies. EXAFS gives detailed information about atomic distances, coordination number and species of the neighboring atoms of the absorbing atom. EXAFS is element-specific method where a core level electron absorbs energy of an incident X-ray photon which results in the formation of a photoelectron which is emitted. An absorption edge can be observed in measurements when the energy of an X-ray photon corresponds to the binding energy of the core level electron. Possible neighboring atoms may cause scattering of the already emitted photoelectrons by the absorbing atom, if the absorbing atom will reabsorb the scattered photoelectron it will affect its absorption coefficient (Newville, 2004). Spectroscopic speciation investigations for neptunium(V) uptake by montmorillonite has been done by Wendt (2009). These EXAFS results suggested the formation of an inner-sphere complex on the montmorillonite surface.

2.1 Material characterization

2.1.1 Montmorillonite

The montmorillonite purified from Wyoming Volclay MX-80 bentonite used in this study was used as received from B+Tech Oy. X-ray diffraction (XRD) experiments were performed for the montmorillonite to study the potential presence of impurities in the mineral. The montmorillonite was found to contain small amounts of quartz and paragonite, which could have been transferred from MX-80 bentonite during purification (Kumpulainen and Kiviranta, 2010). Microelectrophoresis (Zeta Sizer Nano, Malvern Instruments) was used to measure the surface ζ-potential of 0.25 g/l montmorillonite in 10 mM NaCl suspension under N_2-atmosphere. A constant negative charge throughout the investigated pH range (3 – 11) was observed, i.e. no isoelectric point (IEP) could be assigned to the material. The specific surface area of montmorillonite was measured with the N_2-BET technique, and was found to be 49.8 m^2/g. Characterization data on all materials are listed in Table 1.

Table 1. Characterization data on montmorillonite, MX-80 bentonite, Kuru grey granite, and corundum.

	Montmorillonite	**MX-80 bentonite**	**Kuru grey granite**	**Corundum**
IEP [NaCl]	constant negative charge*	-	8 – 9***	8.8**
specific surface area [m^2/g]	49.8*	28.9*	-	14.5**
grain size [µm]	-	-	100 – 1000*	150 – 200**

* This study
** Kupcik et al., 2016
*** Charalambos P., 2001; Chen T. et al., 2013

2.1.2 Bentonite colloids

Bentonite colloids were prepared from Wyoming Volclay MX-80 bentonite which has been shown to consist of 79.1% smectite, 7.5% muscovite, 4.4% quartz, 3.1% calcite, 1.7% plagioclase and other minor impurities (Kumpulainen and Kiviranta, 2010). The

N_2-BET technique was used to define the specific surface area of bentonite and it was found to be 28.9 m^2/g.

The colloid solutions were prepared by mixing 5 g of solid MX-80 bentonite powder with 500 ml of 10 mM $NaClO_4$. The suspensions were allowed to equilibrate for 7 days under shaking before separating colloids from the suspension. Separation was done by centrifuging the suspension for 20 min at 12000 × g (12000 rpm) and the remaining colloid size fraction was measured with Photon Correlation Spectroscopy (PCS). The mean size was found to be approximately 200 – 300 nm. In experiments where a constant pH was required, the colloid suspensions were prepared by buffering the 10 mM $NaClO_4$ to pH 8, 9 or 10 with 10 mM TRIS (tris-hydroxymethyl-aminomethane, pH 8) or CHES ((cyclohexylamino)ethanesulfonic acid, pH 9 and 10).

2.1.3 Corundum

Corundum (α-Al_2O_3) was provided by Taimei Chemicals Tokyo, Japan (TAIMICRON-DAR). The surface area for corundum was found to be 14.5 m^2/g, more detailed characterization data is compiled in Kupcik et al. (2016). Corundum was used as received in this study.

2.1.4 Kuru gray granite

The Kuru gray granite was provided by Kuru Quarry, Tampereen kovakivi Oy, and has been characterized in Hölttä et al. (2004; 2008). The Kuru gray granite consists of 36% potassium feldspar, 35% quartz, 21% plagioclase, 8% amphibole and micas. The total porosity of the granite was found to be 0.47% in Jokelainen et al. (2009). For the neptunium(V) batch sorption experiments, the granite was crushed and sieved so that the final particle size was ranging from 0.1 to 1 mm in diameter. For column experiments, an intact drill core column was used.

2.2 Paper I: Neptunium(V) uptake by montmorillonite and corundum

2.2.1 Sorption and desorption studies

The uptake of neptunium(V) by montmorillonite and corundum was investigated in Paper I. The batch sorption studies described in this paragraph were modeled using DDL model and the speciation of actinide on the two mineral surfaces were investigated with ATR FT-IR and EXAFS spectroscopies (see section 2.2.2).

Neptunium uptake by montmorillonite was investigated in carbonate free conditions in order to exclude the formation of neptunium-carbonato complexes that influence the uptake and speciation of neptunium on the mineral surface. Comparative sorption studies were conducted with corundum to elucidate the role of aluminol groups in the sorption reaction. The background electrolyte for all of the sorption experiments was 10 mM $NaClO_4$ and the neptunium concentration in the experiments (excluding the isotherms) was 10^{-6} M. For the isotherm investigations, a constant pH was achieved with buffer solutions tris-hydroxymethylaminomethane (TRIS, pH 8) and N-cyclohexyl-2-aminoethanesulfonic acid (CHES, pH 9 and 10). The sample pH was adjusted with 0.01 – 1 M $HClO_4$ and NaOH solutions. The neptunium concentration for isotherms ranged from 0.001 to 5 µM. The solid was separated from the liquid either after 7 or 30 days equilibrium time and a one milliliter aliquot was taken for liquid scintillation counting (LSC). The amount of sorbed neptunium was measured with LSC (Tri-Carb 3100 TR or Quantulus) using α/β-discrimination to separate out the β disintegrations from the Np-237 daughter nuclide Pa-233.

Neptunium uptake by montmorillonite was investigated as a function of pH, neptunium concentration, time, and solid concentration. Samples were prepared by adding neptunium and a small aliquot of concentrated montmorillonite solution (2.5 or 20 g/l in 10 mM $NaClO_4$ so that the final concentration of 0.5 or 5 g/l was achieved) in polypropylene tubes or polyethylene vials. The pH in the neptunium experiments ranged from 4 to 11. The solid phase was separated from the liquid by centrifugation (min. 3080 g/60min) either after 7 or 30 days of equilibration time.

Neptunium uptake by corundum was investigated using only one solid concentration of 0.5 g/l and as a function of pH. Additional isotherm experiments were performed…. The corundum investigations were minor due to existing batch sorption and isotherm data that can be found in Virtanen et al. (2016).

Neptunium(V) desorption was investigated in two different experimental set-ups in similar experimental conditions where the sorption experiments had been performed i.e. neptunium concentration of 10^{-6} M, solid to liquid ratio of 5 g/l, 10 mM $NaClO_4$ as background electrolyte and equilibration time of 7 days. First experiments were

conducted for both montmorillonite and corundum at pH 8, 9 and 10, after equilibration time of 7 days, the background electrolyte was exchanged to a fresh one on every 2 – 3 days. These experiments simulate the final phase in ATF FT-IR spectroscopy studies where the mineral film is being flushed with blank solution after sorption phase. Second desorption experiment was done only for montmorillonite, in this experiment, after 7 days of equilibration; the pH was decreased to 5. Desorption was followed from one hour up to 15 days, the purpose of this experiment was to compare whether the sorption and desorption kinetics are the same.

2.2.2 Spectroscopic speciation studies

Batch sorption studies alone are not sufficient to give detailed information about the actual surface complexation on water-mineral surface, spectroscopic methods are essential while investigating surface processes (Lefevre, 2004). Thus, the sorption of neptunium(V) on montmorillonite and corundum was investigated with ATR FT_IR and EXAFS spectroscopies.

In the present work Infrared spectra were measured from 1800 to 600 cm^{-1} on a Bruker Vertex 70/v vacuum spectrometer, equipped with a Mercury Cadmium Telluride (MCT) detector. The spectral resolution was 4 cm^{-1} and spectra were averaged over 256 scans. A horizontal diamond crystal with nine internal reflections (DURA SamplIR II, Smiths Inc.) was used. The mineral film was prepared by pipetting either corundum or montmorillonite suspension on top of ATR diamond crystal, and allowing he mineral film to dry under gentle nitrogen flow. The procedure was repeated until the average mass density reached 0.2 mg/cm^2. Preconditioning of the mineral film was performed by flushing the mineral film with blank solution (0.01 M NaCl, pH 10) for 60 minutes using a flow cell at a flow rate of 100 µl/min. In the following sorption step, the mineral film was flushed for 120 min with 0.01 M NaCl (pH 10) solution containing neptunium(V). During the final conditioning step, the mineral film was flushed for 60 min with a blank solution (0.01 M NaCl, pH 10) to see if desorption occurs. Due to overlapping of vibrational regions for H_2O and NpO_2^+, all solutions were prepared in deuterated water (D_2O).

The XAS samples were prepared in 10 mM NaCl at pH 9 or 10 using 5 g/l corundum or montmorillonite and 20 µmol/l neptunium(V) concentrations. After equilibration time of one week, the solid phase was separated from supernatant by centrifugation at 3830 g (6000rpm/60min). The solid phase was transferred to a Teflon sample holders which were sealed with Teflon lids. Sample preparation was performed under N_2-atmosphere and stored in liquid nitrogen until XAS measurements.

Both XANES and EXAFS were collected at the Rossendorf Beamline (ROBL) at the European Synchrotron Radiation Facility (ESRF). Np L_{III}-edge was measured utilizing a Si(111) double-crystal monochromator under ring operating conditions of 6 GeV and 150 – 200. X-rays were collimated with a flat meridionally-bent 140-cm long Rh-coated silicon mirror. The spectra were collected at 15 K in fluorescence mode with gas-filled ionization chambers and a 13-element solid state detector (I_F, Canberra). Energy calibration of the collected spectra was performed by the simultaneous measurement of reference Y foil. At minimum average of four spectra were gathered for further analysis. Data was analyzed with WinXAS (version 3.2) following standard procedure (Koningsberger and Prins, 1988). EXAFS theoretical fitting was performed both in *k*-space and *R*-space. EXAFS theoretical phase and amplitude required for the theoretical fitting were calculated by the programme code FEFF 8.20 (Ankudinov et al., 1998) based on the hypothetical cluster "hydrated $Np^{V}O_2^+$ sorbed on gibbsite" employed by Gückel et al. (2013) and Virtanen et al. (2016). The threshold energy, $E_{k=0}$, was defined at the first XANES inflection point of each spectrum. The amplitude reduction factor,S_0^2, was fixed at 0.9, while the shifts in $E_{k=0}$ were varied but constrained to the same value for all the shells.

2.2.3 Surface complexation modeling

The surface complexation modeling was done for neptunium(V) batch sorption experiments on montmorillonite using a rather simple Diffuse Double Layer (DDL) model. The model was applied using PHREEQC (version 3.1.5-9113) (Parkshurst and Appelo, 2013) coupled with the software UCODE2005 (Poeter et al., 2006). Parameters used in the surface complexation modeling were surface site density (SSD = 6.24 × 10^{-5} mol/g mineral), surface protolysis constants ($\log K_{a1}$ = -6.05, $\log K_{a2}$ = -

7.79) and specific surface area (A_s = 49.8 m^2/g). IEP point of 6.92 was calculated using above mentioned protolysis constants.

2.3 Paper II: Neptunium(V) uptake by bentonite colloids and Kuru gray granite

2.3.1 Batch sorption studies

In Paper II the focus of the sorption investigations was to elucidate the role of bentonite colloids on the migration of neptunium(V) in granitic rock under stagnant (batch type experiments) and flowing water (column experiments) conditions.

The neptunium uptake studies by bentonite colloids were conducted both in N_2– and open atmosphere. The experiments under N_2 atmosphere were conducted similarly to the montmorillonite experiments described above, while the studies at ambient conditions were conducted to support the column experiments (see section 2.3.1) which were conducted without the exclusion of atmospheric CO_2. Colloid solutions were prepared from the MX-80 bentonite under constant rotation for 14 days and the colloidal phase was separated from the solid by centrifugation (12 000 g/20 min). The colloid solutions were directly prepared into the final background electrolyte of $NaClO_4$, TRIS buffered $NaClO_4$ (pH 8) or CHES buffered $NaClO_4$ (pH 9 and 10). The colloid concentration for the pH-edge in N_2-atmosphere was 0.08 g/l and in open atmosphere 0.8 g/l, and the investigated pH range was from 4 to 11. The isotherm investigations were conducted only in N_2-atmosphere at pH 8, 9, and 10 with colloid concentrations of 0.1 g/l, 0.06 g/l and 0.2 g/l, respectively.

As the column experiments were conducted under ambient atmosphere the neptunium uptake investigations by crushed Kuru gray granite were also conducted under ambient atmosphere. The solid content of crushed Kuru gray granite was 40 g/l in each sample and neptunium uptake by Kuru gray as a function of pH was investigated in the range from 4 to 10.

2.3.2 Column experiments

Column experiments were conducted in order to investigate the influence of bentonite colloids on neptunium(V) migration. Experiments were conducted under flowing water conditions in a 28 cm long drill core column with a diameter of 1.4 cm,

which was placed in a 30 cm long Glass Econo-Column with a diameter of 1.5 cm. Thus, the gap between the intact drill core column and the glass tube formed a 0.1 cm flow channel resulting in total liquid volume of 6.4 ml in the column. The height of the column was adjusted with a Bio-Rad Flow Adaptor. The drill core column has been preconditioned by ultrasonicating in ethanol to remove any dust or other remnants of the drilling procedure. The experimental set-up in the absence of colloids consisted of a background electrolyte which was continuously pumped through the column. In the presence of colloids the background electrolyte solution was exchanged to a solution containing bentonite colloids. An injector loop of known volume (12 µL) was used to inject the tracer (either Np-237 or Cl-36) into the column. The flow direction in the drill core column was from bottom to top in order to exclude effects of gravitation. Breakthrough of the tracer was determined by using a fraction collector. Earlier, the same intact drill core column was used in parallel in block-scale experiments (Hölttä et al., 2008) where flow rates 0.3 and 0.8 ml/h were used, thus, the same flow rates were used in this study. A conservative tracer (Cl-36) was used to determine flow properties of the drill core column. Concentration used for Cl-36 was 8.7×10^{-2} M which despite the high concentration dilutes fast in the total column volume of 6.4 ml, and is diluted by a factor of ten in the first 0.5 cm.

For neptunium(V) column experiments, a concentration of 2×10^{-4} M was used. This concentration is diluted in the first 2 cm of the column to highest concentration used in the isotherm experiments (5×10^{-6} M). Column experiments with neptunium were performed both in the presence and absence of bentonite colloids of concentration varying between 0.08 and 0.32 g/l.

Column experiments were conducted at two different flow rates 0.8 and 0.3 ml/h in order to investigate the influence of sorption kinetics on neptunium(V) breakthrough. For environmental conditions i.e. pH, pH 8 and 10 were chosen based on batch sorption experiments for montmorillonite extracted from MX-80 bentonite.

2.3.3 Analytical modeling of column experiments

The breakthrough curves of chloride and neptunium(V) from the intact drill core were modeled using the analytical solution of advection-matrix diffusion equation in

cylindrical coordinates. The used model takes into account 1D diffusion in the flow field in direction of advection, 1D radial diffusion in the rock matrix, sorption on mineral surfaces in the rock matrix and the channeled flow field between the cylindrical sample and the pipe surrounding the sample.

3 RESULTS

3.1 Batch sorption investigations of neptunium(V) uptake by EBS constituents

3.1.1 Sorption in the absence of carbonates

Adsorption

The adsorption of neptunium(V) on corundum, montmorillonite, and bentonite colloids was investigated in the absence of carbonates (Papers I and II). Neptunium(V) uptake curves as a function of pH are shown in Figure 3 for all three materials.

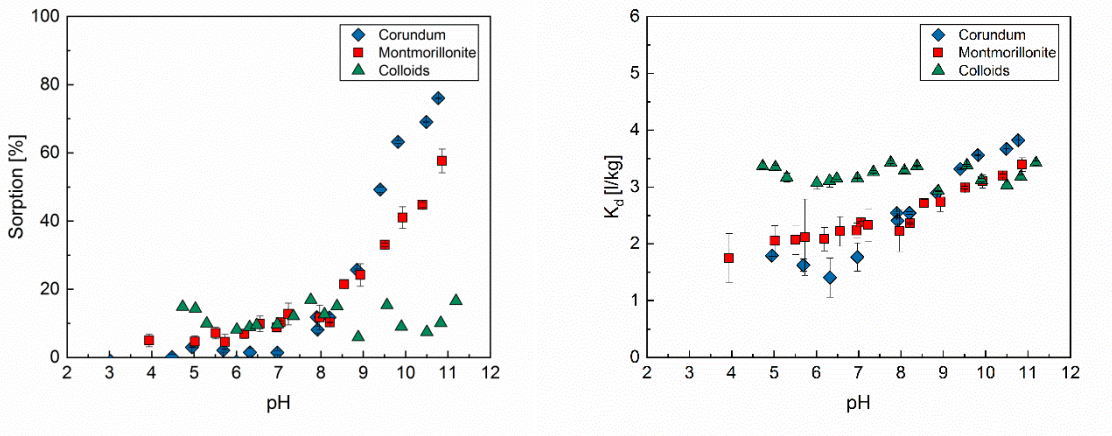

Figure 3. Neptunium(V) uptake by montmorillonite, bentonite colloids and corundum as a function of pH after 7 days equilibration. Figures above are presented as log K_d (l/kg) and figures below as adsorption percentages. Neptunium(V) concentration 10^{-6} M in 10 mM $NaClO_4$ and equilibration time of 7 days.

After 7 days of equilibration, neptunium(V) uptake by corundum and montmorillonite show increase in sorption at pH 7 and higher (Fig. 3). Neptunium(V) uptake by bentonite colloids remains constant at 7 – 15% throughout the investigated

pH range. The pH-edge for neptunium(V) uptake by bentonite colloids does not show similar behavior as for montmorillonite and corundum where a significant increase in sorption can be seen at pH 7. Neptunium(V) sorption on bentonite colloids is not pH dependent indicating that the sorption mechanism is not the same inner-sphere complex nature as suggested for corundum and montmorillonite based on the spectroscopic investigations later discussed in section 3.2 At pH 8, neptunium(V) sorption by both montmorillonite and corundum increase sharply indicating deprotonation of the aluminol groups on the mineral surface and adsorption of neptunium(V). For montmorillonite, a constant sorption of approximately 10% is seen at pH below 7. Such behavior cannot be observed for corundum, which has a rather high IEP at 8.8. The negatively charged planar sites of montmorillonite attract positively charged neptunyl cation, and neptunium(V) is sorbed by ion exchange under acidic conditions.

Neptunium(V) uptake by montmorillonite, corundum and bentonite colloids was also investigated as a function of neptunium(V) concentration to gain more information about the nature of the sorption sites. The isotherm results at are presented in Fig 4.

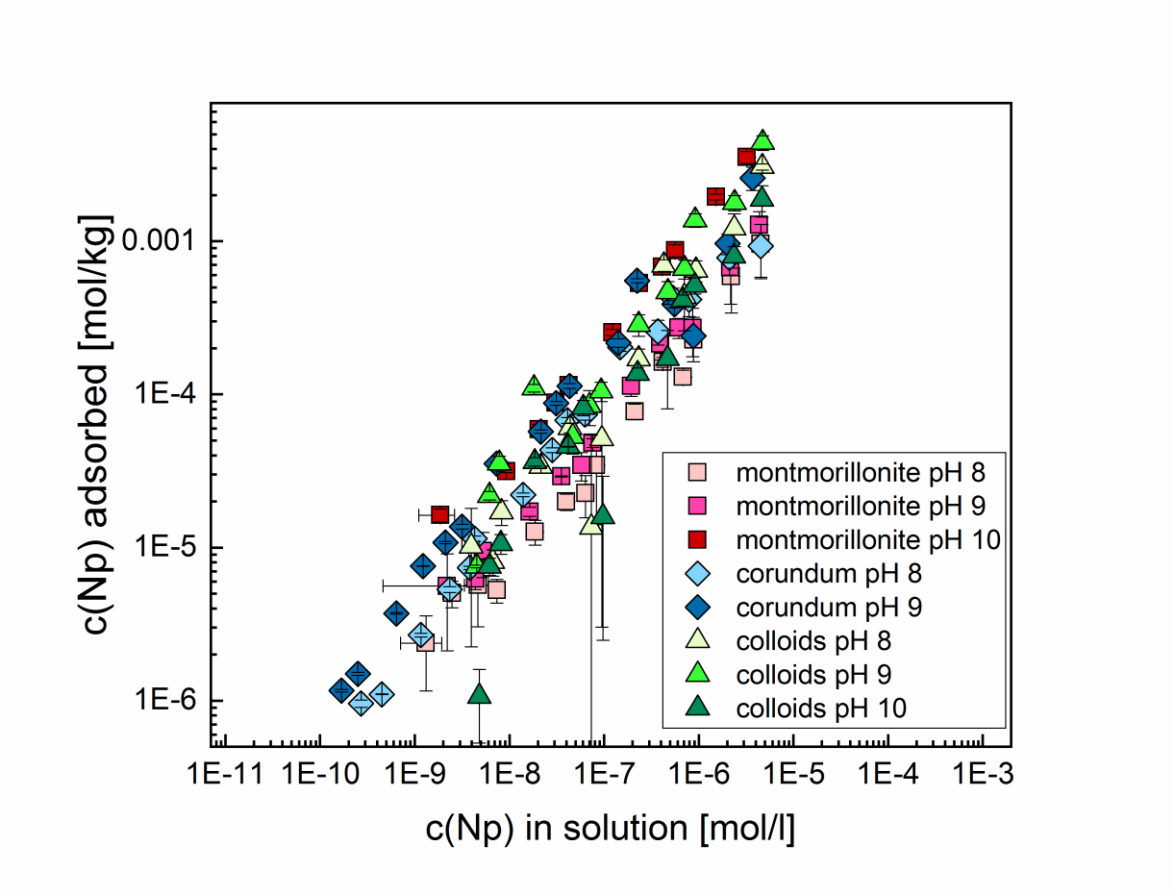

Figure 4. Neptunium(V) uptake by montmorillonite, corundum and bentonite colloids as a function of neptunium(V) concentration 10^{-9} – 5 × 10^{-6} M at pH 8 and 9 for corundum, and pH 8, 9 and 10 for montmorillonite and bentonite colloids. Background electrolyte was 10 mM $NaClO_4$ in 10 mM TRIS (pH8) or 10 mM CHES (pH 9 and 10).

Isotherms for montmorillonite, corundum and bentonite colloids are all linear with a slope of approximately 1 indicating that at pH 8, 9, and 10, only one type of sorption site is available in each experiment. As the pH increases, the sorption isotherms for montmorillonite and corundum shift to towards higher sorption on the mineral surface. This behavior is well in accordance with the uptake experiments performed as a function of pH (Fig. 3). Neptunium(V) uptake by bentonite colloids behaves similarly at pH 8 and 9, however, the sorption isotherm at pH 10 shows less sorption capacity than the one performed at pH 8. This could be due to different colloids concentration used in the colloids solution and inaccuracy of the colloid concentration calibration curve (Paper II). Sorption sites can be divided into strong

and weak sorption sites, cation exchange can be considered as weak sorption mechanism, and surface complexation as strong sorption mechanism. In Fig. 3 for corundum and montmorillonite, a sharp sorption edge can be seen at approximately pH 7, indicating dominance of strong sorption sites, this behavior cannot be seen for bentonite colloids. The constant neptunium(V) uptake by bentonite colloids throughout the investigated pH range indicates that weak sorption sites, i.e. cation exchange, are responsible for neptunium(V) uptake by bentonite colloids. The linear shape of the isotherms for all minerals indicate that only one type of surface site is responsible for neptunium(V) uptake. Therefore, formation of a strong sorption complex on the colloid surface is unlikely.

Desorption

Desorption of neptunium(V) from montmorillonite and corundum simulating flowing background electrolyte conditions was investigated in desorption experiments (Paper I).

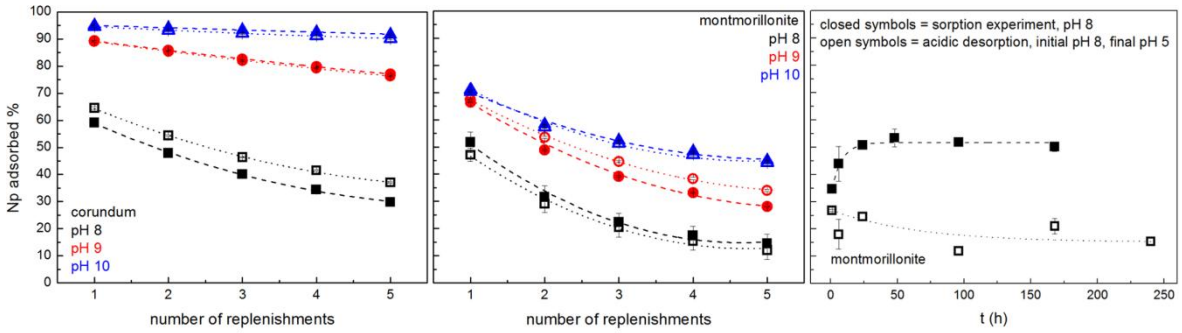

Fig. 5. Neptunium(V) replenishment experiments as adsorption percentage after replacing the background electrolyte every 2 – 3 days from corundum (left) and montmorillonite (middle) at pH 8, 9 and 10. Kinetic sorption (closed symbols) and acidic desorption (open symbols) experiments of neptunium(V) as a function of time (right). Neptunium(V) concentration 10^{-6} M in 10 mM $NaClO_4$.

Fig. 5. (left and middle) shows the results of the desorption replenishment experiments where the background electrolyte was exchanged every 2-3 days (open symbols) or every 7 days (closed symbols) for corundum and montmorillonite. For both minerals the extent of desorption decreases as the pH increases, indicating the formation of a surface complex at higher pH which is more tightly bound on the mineral surface than at more acidic conditions. For corundum, the extent of desorption was independent from the exchange interval of either 2 – 3 or seven days at all investigated pH conditions. For montmorillonite, neptunium(V) was found to desorb by 75% at pH 8 independent of the exchange interval. At pH 9, a difference between two different exchange intervals could be seen as the extent of desorption for the 7 day exchange interval is slightly higher. The desorption studies clearly show that neptunium(V) uptake by the investigated minerals is reversible, even at alkaline conditions. The pH-dependent differences in the desorption behavior further imply that different surface complexes with differing desorption kinetics form on the mineral surfaces. Formation of two different surface complexes is supported by the ATR FT-IR studies and surface complexation modeling as later discussed in section 3.3. No influence of the exchange interval could be seen for neptunium(V) desorption at pH 10.

The results of the acidic desorption experiments show that a constant sorption of approximately 15% was obtained after 50 hours acidifying the sample (Fig. 5, right). This behavior where neptunium(V) no longer desorbs from the montmorillonite surface after reaching plateau at 15% is an indicator of ion exchange.

3.1.2 Sorption in the presence of carbonates

Neptunium(V) uptake by bentonite colloids and crushed granite in the presence of carbonates was investigated to simulate the column experiments that were conducted under the same conditions (Paper II).

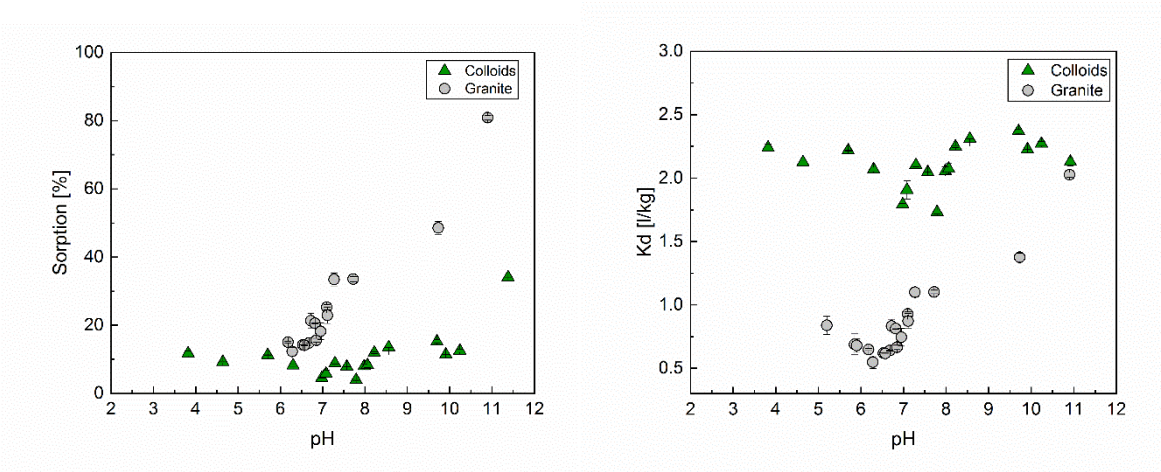

Fig 6. Neptunium(V) uptake by MX-80 bentonite colloids and crushed granite as a function of pH under ambient atmosphere. Results presented as sorption percentage (left) and as K_d m^3/kg (right). Neptunium(V) concentration 10^{-6} M in 10 mM $NaClO_4$ and equilibration time of 7 days.

In Fig. 6 and 3, no difference can be seen between neptunium(V) uptake by bentonite colloids under N_2- and ambient atmosphere, indicating that neptunium(V) carbonate complex can be excluded from the column experiments performed at pH 8 and 10. The difference in the K_d values under ambient and N_2-atmosphere can be explained with the inaccuracy of the calibration used to calculate curve colloid concentrations below 1 g/l, used colloid concentrations were 0.08 g/l for N_2 and 0.8 g/l for ambient atmosphere. Unlike neptunium(V) uptake by montmorillonite and corundum, no increase in sorption can be seen throughout the pH range where sorption remains constant.

In Fig. 6. for crushed granite, pH dependent sorption can be seen above pH 7, however, the overall sorption percentage of 80% and K_d of 0.1 m^3/kg remain rather low. Reduction of neptunium(V) reduction into neptunium(IV) is not observed in this study as it has been seen in other studies investigating neptunium(V) uptake by granite (Kumata and Vandergraaf, 1998; Kienzler et al., 2003; Park et al., 2012). The pH dependent sorption of neptunium(V) onto crushed granite was used to select the experimental conditions for column experiments based on the Bolzmann fit on the neptunium(V) sorption onto crushed granite as a function of pH.

3.2 Spectroscopic investigations of neptunium(V) sorption on montmorillonite and corundum

3.2.1 ATR FT-IR spectroscopy

ATR FT-IR spectroscopy is based on changes in absorption on the mineral film. Since inner-sphere complex formation includes a change in the actinide coordination, a change in position of the absorption band can be seen. Outer-sphere complexation does not include changes in the coordination chemistry, thus absorption band does not differ significantly from the one originating from the mobile actinide cation. ATR FT-IR spectroscopy provides information about the sorption process *in situ* and under flowing background electrolyte conditions. These results can be compared with the batch desorption studies were the background electrolyte was changed regularly to simulate flowing background electrolyte conditions. The behavior of neptunium(V) in these studies give an prediction how neptunium(V) behaves in the column experiments. Time resolved infrared spectra of neptunium(V) sorption on corundum (A) and montmorillonite (B) are presented in Fig 7 (Paper I).

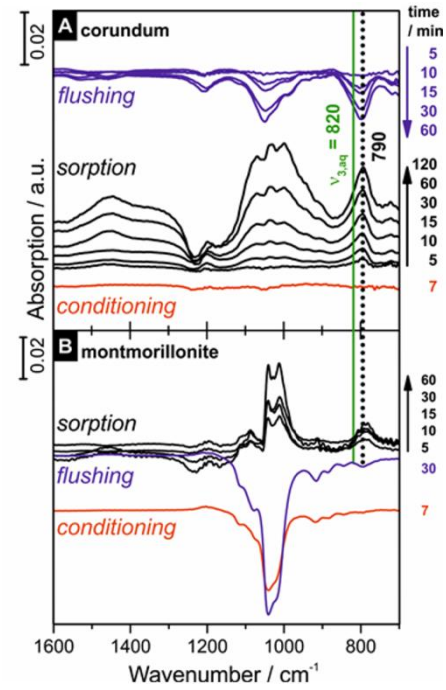

Fig. 7. *In situ* time resolved ATR FT-IR spectra of neptunium(V) sorption on corundum (A) and montmorillonite (B) at pH 10. Red traces for the first step "conditioning", black traces for the second step "sorption" and blue traces for final step "flushing".

Neptunium(V) concentration 50 μM, 0.01 M NaCl in D_2O, N_2-atmosphere and mineral concentration of approximately 0.2 mg/cm^2.

For corundum, a stable mineral film throughout the experiment, indicated by the constant baseline, was obtained (Fig. 7, A, red traces). For montmorillonite, a strong negative vibration can be seen at approximately 1100 cm^{-1} which can be attributed to vibrations of the silanol groups on the montmorillonite surface (Fig. 7, B, red traces). The negative peak is larger at the final step of flushing, indicating that montmorillonite is slowly removed from the mineral film during the experiments. However, the difference between the initial and final mineral film spectra is only 5%. An absorption band at 790 cm^{-1} can be attributed to the antisymmetric stretching mode ν_3 of adsorbed neptunium(V). The rather large shift of this stretching mode in comparison to the neptunium aquo ion at 820 cm^{-1} (Jones and Penneman, 1953, Müller et al., 2009; 2015), is an indication of inner-sphere complex formation No other absorption bands can be seen for the minerals, indicating that only one surface species is present. Surface sites for corundum and montmorillonite are saturated after 60 and 15 minutes, respectively. During the final flushing step, surface species that are easily removable can be observed. The absorption band at 790 cm^{-1} vanished for both minerals, indicating that complete desorption of neptunium(V) has occurred. For corundum this was not expected as the desorption experiments did not show significant desorption from the mineral surface. Thus, the experimental conditions in the desorption studies do not fully describe the experimental set-up in ATR FT-IR experiments where the mineral film was constantly flushed by the background electrolyte. Similar desorption of inner-sphere bound neptunium(V) from TiO_2 and $Al(OH)_3$ surfaces was not observed by Müller et al. (2009) and Gückel et al. (2013). In the study by Müller et al. (2015) neptunium(V) uptake by hematite was investigated and similar desorption of neptunium(V) was seen as in this study. The slight tailing seen at the neptunium(V) ν_3 stretching for montmorillonite could be an indicator of another surface complexation species. However, the relatively low sorption percentage of neptunium(V) and high absorbing background generated by the functional surface groups of montmorillonite hamper the resolution of the ATR FT-IR spectra. Due to the high removal of neptunium(V) from the montmorillonite surface under flowing water conditions, our desorption and ATR-FT-IR experiments serves as

a first indication of a low adsorption, and subsequently small influence of mobile colloids under flowing water conditions, as discussed in section 3.4.

3.2.2 X-ray absorption spectroscopy

EXAFS provides detailed information about the coordination chemistry, bond lengths, neighboring atoms and oxidation state of the actinide complex on mineral surface. In this study, EXAFS samples and the speciation studies were performed for both montmorillonite and corundum. XAS measurements for montmorillonite showed a zirconium impurity, which is interfering with the neptunium(V) EXAFS region. The Np L_{III}-edge XAS spectra for montmorillonite is presented in Fig 8.

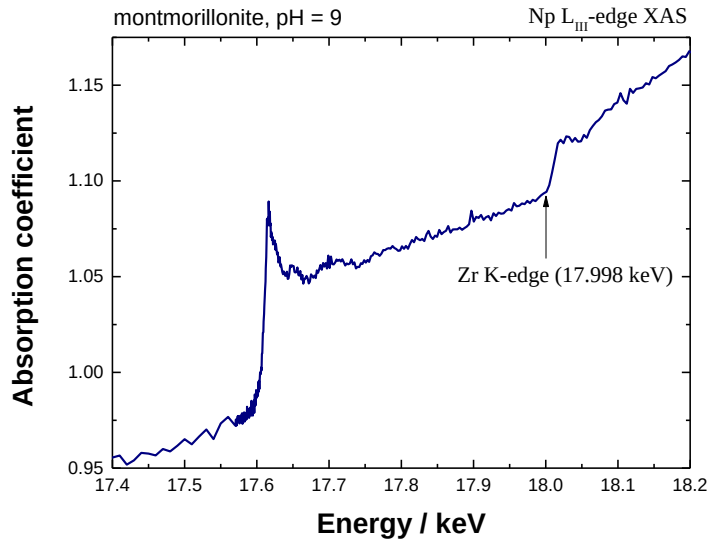

Fig 8. Neptunium(V) L_{III}-edge XANES spectra for neptunium(V) adsorbed on montmorillonite and the zirconium impurity Zr K-edge (17.998 keV) at pH 9.

Due to this zirconium impurity on montmorillonite, further EXAFS measurements were performed for corundum only. The EXAFS spectra for corundum samples at pH 9 and 10 and their corresponding Fourier transforms (FTs) are presented in Figure 9.

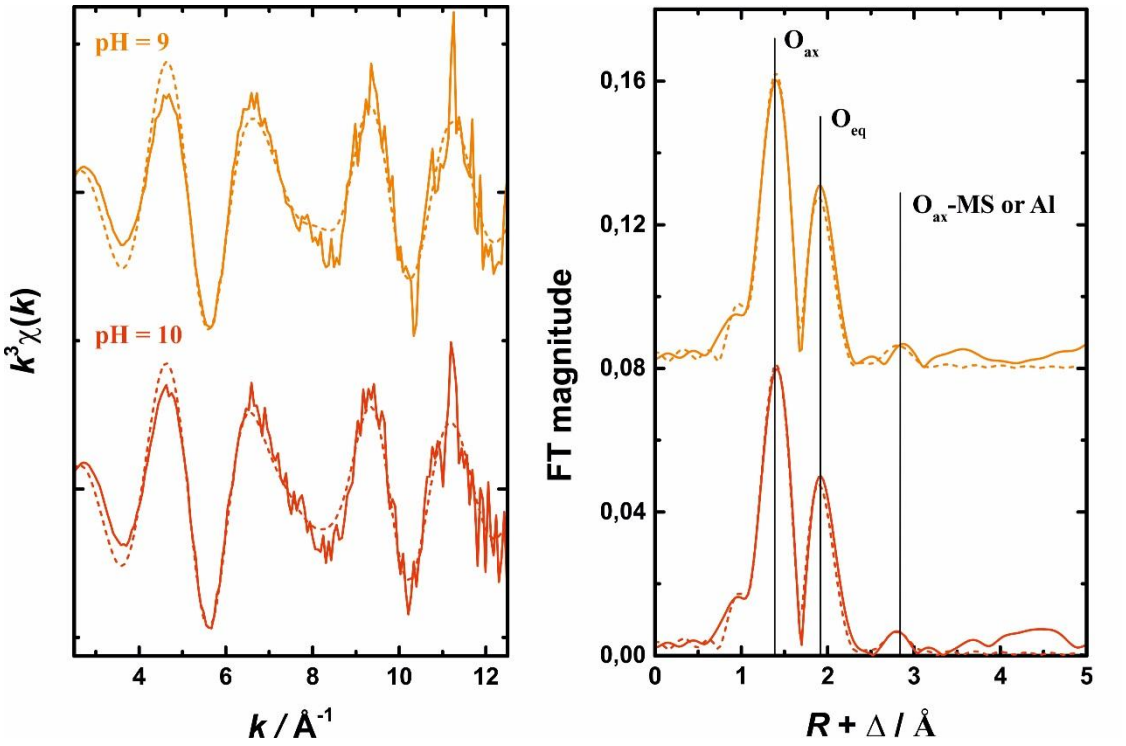

Fig. 9. k^3-weighted Np L_{III}-edge XANES spectra for neptunium(V) adsorbed on corundum at pH 9 and 10 (left) and the corresponding Fourier transforms (right). Solid line presents the measured data and dashed lines theoretical fitting. Phase shifts are not corrected in the FT's.

It can be seen in Fig. 9 that the prevailing neptunium species was confirmed by shoulder at 17.63 keV of the Np L_{III}-edge XANES spectra for corundum. This characteristic shoulder is originating from the trans-dioxo arrangement of neptunyl ion in the samples (Soderholm et al., 1999), thus confirming that neptunium is in its' pentavalent form. The EXAFS theoretical curve fitting resulted in highest FT peak at $R + \Delta = 1.4$ Å which can be attributed to the two axial oxygens of the neptunium(V) cation. The second FT peak at $R + \Delta = 2.0$ Å was assigned as ligand coordination in the equatorial plane of the neptunium(V) cation (Ikeda-Ohno et al., 2008). The EXAFS samples contained only water, NaCl, corundum and neptunium(V), thus, possible ligands could be neptunium(V) hydroxide complexes. However, the ATR FT-IR studies did not imply existence of such complexes, and formation of neptunium(V) hydroxide complexes at pH 10 is unlikely (Müller et al., 2015). Neptunium(V) complexation with Cl^- in these experimental conditions has been proven to be negligible (Allen et al., 1997) which leaves water and aluminol surface groups on corundum surface as

possible ligands for neptunium(V). EXAFS theoretical fitting resulted in interatomic distances of 1.86 Å (Np-O_{ax}) and 2.45 – 2.46 Å (Np-O_{eq}), this is well in agreement with results obtained for neptunium(V) adsorption on gibbsite (Gückel et al., 2013). The third peak in the theoretical FT fitting could be either single scattering of Al on corundum surface or multiple scattering from linear O_{ax}-Np-O_{ax} neptunium cations, which is in agreement with neptunium(V) sorption on gibbsite (Gückel et al., 2013) and hematite (Arai et al., 2007). A possible edge-sharing neptunium(V) species on corundum surface would result in Np – Al distance of 3.33 – 3.38 Å.

3.3 Surface complexation modeling

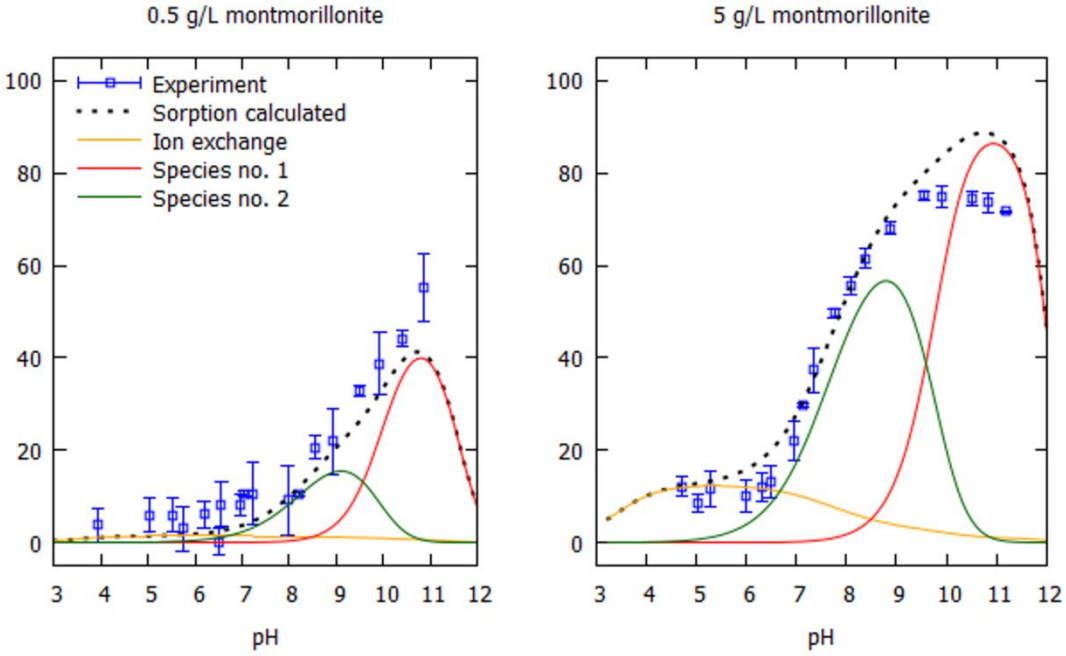

Fig. 10. Modeling results for neptunium(V) uptake by montmorillonite at two different solid to liquid ratios 0.5 g/l (left) and 5 g/l (right) as a function of pH in 10 mM $NaClO_4$.

In Fig. 10 the modelling results for the experimental data of neptunium(V) uptake by 0.5 g/l and 5 g/l montmorillonite as a function of pH is shown. Ion exchange reaction following the Gaines-Thomas convention as implemented in PHREEQC (Appelo and Parkhurst, 2013) was used for fitting the sorption data below pH 7.2 where constant sorption by ion exchange was observed. For the second step, sorption edges for both 0.5 and 5 g/l montmorillonite in 10 mM $NaClO_4$ a bidentate surface complexation

reaction supported by the spectroscopic speciation studies was used. At first, fitting was performed using a monodentate surface complex, however, this did not fit the sorption data, and was further not supported by the spectroscopic speciation studies. For successful fitting, ion exchange and two pH dependent surface species were needed. The first species could be assigned as the bidentate inner-sphere complex supported by both ATR FT-IR and EXAFS data. The second species, which did not require deprotonation of functional surface groups a, was not supported or implied by the spectroscopic investigations, however, it was necessary for surface complexation modeling. This species could be assigned as an outer-sphere complex and it was supported by the slight tailing seen in the ATR FT-IR absorption band.

3.4 Column experiments

In Paper II, Neptunium(V) uptake by crystalline granitic rock and bentonite colloids was investigated under stagnant conditions in batch-type experiments and the role of stable and mobile bentonite colloids on the migration of neptunium(V) through intact granite rock columns was investigated under flowing water conditions. The column experiments were performed in a Kuru gray granite column under ambient air both in the absence and presence of bentonite colloids. The flow through properties of the drill core column were investigated by following the migration of a conservative chloride tracer through the column.

3.4.1 Cl-36

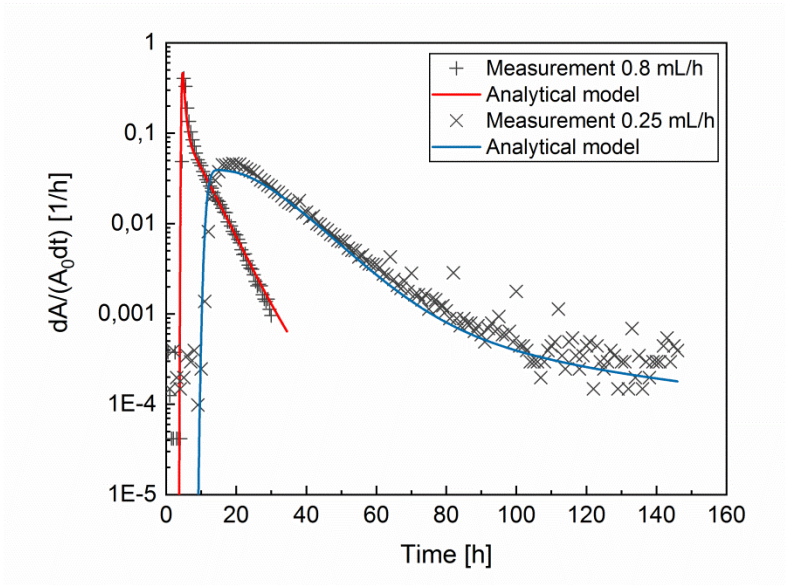

Fig. 11. Measured (symbols) and modeled (solid line) breakthrough curves of Cl-36 through intact drill core column in the absence of bentonite colloids. The chloride concentration in the injected tracer volume was 8.7×10^{-2} M.

The flow through properties of the intact Kuru grey granite column was investigated using a conservative tracer Cl-36 at to different flow rates, 0.8 and 0.25 ml/h, to mimic the experimental set-up for neptunium(V) and bentonite colloid break through. In Fig. 9 the breakthrough of Cl-36 is depending on the flow rate as expected, slight tailing for both curves can be seen. Similar behavior has been observed by Park et al. (2012) where tailing was assigned to dispersion in the column. The velocity scaling is not constant between all measurements, indicating that the intact drill core column has been slightly displaced in the glass tube, which further influences the flow paths.

3.4.2 Neptunium(V) and colloids

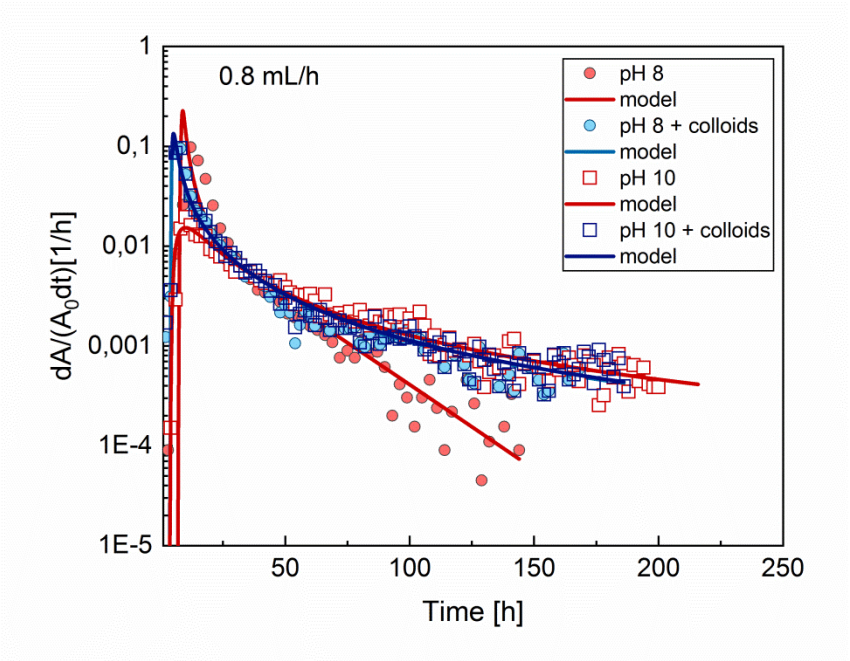

Fig. 12. Measured (symbols) and modeled (solid lines) breakthrough curves of neptunium(V) through intact drill core column in the absence (red symbols) and presence (blue symbols) of bentonite colloids at pH 8 (solid symbols) and 10 (open symbols).

Neptunium(V) migration in the Kuru grey intact drill core column in the absence and presence of bentonite colloids at two different flow rates, 0.3 and 0.8 ml/h, and pH 8 and 10 are shown in Fig. 12. The colloid breakthrough was determined from the neptunium(V) experiment in the presence of colloids only at pH 8 and a flow rate of 0.3 ml/h. For other neptunium(V) breakthrough experiments in the presence of bentonite colloids at pH 8, 0.8 ml/h and pH 10, 0.3 ml/h, the colloid breakthrough curves were measured in separate experiments without the presence of neptunium(V). The colloid recovery for the flow rate of 0.8 ml/h was 80 ± 9% throughout the experiments. For the 0.3 ml/h flow rate the colloid recovery was varying between 98% and 65% in the beginning, after 125 hours a decrease in recovery down to 20% can be seen. This implies that colloids are filtered into stagnant areas of the flow channel or tubing. A similar behavior cannot be seen for neptunium(V) indicating that neptunium(V) is migrating in the aqueous phase. For the 0.3 ml/h flowrate, the pre-peak position is approximately 20 h for both experiments in the absence and presence of bentonite colloids. For the higher flow rate the situation is a bit different, the pre-peak position is not constant, indicating that the intact drill core must have moved in the glass column changing the flow environment. Due to neptunium(V) sorption onto Kuru gray granite, the slope for the breakthrough peak is not as steep as for chloride. Similarly for the late breakthrough curve, only matrix diffusion is not sufficient to explain the breakthrough behavior. Sorption at the late breakthrough curve is further supported by the difference between the curves for 0.8 ml/h at pH 8 and 10. The breakthrough peak maximum at pH 10 is not as high as for pH 8, and the neptunium(V) recovery is decreasing slower than that of pH 8. The influence of bentonite colloids on neptunium(V) breakthrough is negligible for both flow rates and at pH 8 and 10. Neptunium(V) uptake by bentonite colloids remained at approximately 10% in the batch sorption experiments, however, for crushed granite batch sorption experiments neptunium(V) uptake by crushed granite increases from approximately 35% to 65%. This significant difference should affect neptunium(V) breakthrough via colloid sorption at pH 10, though no influence of bentonite colloids is seen at the flow rate of 0.3 ml/h. For the lower flow rate no retention of neptunium(V) to the column material can be seen. However, the colloid breakthrough is varying largely in contrast to neptunium(V) indicating that neptunium(V) would be in its aqueous form. Neptunium(V)

breakthrough at flowrate 0.8 ml/h show a difference in the absence and presence of bentonite colloids, for the former, a steeper breakthrough curve can be seen. This is indicating that neptunium(V) retention in the presence of bentonite colloids to the intact drill core column would be higher. This could be explained by colloid sorption onto intact drill core column, providing more sorption sites for neptunium(V), or by clogging colloids could interrupt the flow path of neptunium(V).

4 CONCLUSIONS

In this study neptunium(V) retention on EBS constituents, i.e. bentonite and montmorillonite, the model mineral phase corundum, and granitic rock was investigated by batch type experiments and spectroscopic methods. The influence of bentonite colloids on neptunium(V) migration was investigated by column experiments.

The results showed that neptunium(V) is rather well retained on these solid phases under stagnant water conditions in the alkaline pH range, which is expected to prevail in a final repository for spent nuclear fuel in granitic rock (Hellä et al., 2014). Combined EXAFS studies and modelling result showed that several types of neptunium(V) species co-exist on the clay mineral surface, ranging from cation exchanged neptunium(V) on permanent negative surface groups on the mineral surface to pH-dependent outer-sphere and inner-sphere complexes in the circumneutral to alkaline pH range. Despite the predominance of inner-sphere sorbed neptunium(V) above pH 9, the sorption reaction was found to be highly reversible in combined batch desorption experiments and ATR-FT-IR spectroscopic investigations, simulating flowing water conditions. The reversibility could be confirmed in the column experiments where only a very low amount of neptunium(V) adsorption onto the granitic column material could be observed in the breakthrough curves for various flow velocities despite that a much higher retention of neptunium(V) was obtained in the batch sorption studies under stagnant water conditions. No influence of bentonite colloids on the neptunium(V) breakthrough in the granite columns could be established at these flowing water conditions, most likely due to the low retention

of neptunium(V) on the low amount of colloid material and the high reversibility of the sorption reaction.

The results imply that the crystalline granitic rock and bentonite buffer have a negligible effect on neptunium(V) retardation in case of canister failure and release of neptunium(V) to the flowing groundwater. In stagnant pore waters, neptunium(V) will retain on the solids phases. In addition, the eroding bentonite colloids from the buffer to the groundwater seem to have no enhancing effect on neptunium(V) migration under mildly oxic flowing groundwater conditions in the final repository. This implies that the most important mechanism for neptunium(V) retardation under the above-mentioned conditions in the bedrock is matrix diffusion into the rock matrix.

5 REFERENCES

Allen P. G., Bucher J. J., Shuh D. K., Edelstein N. M. and Reich T., 1997. Investigation of aquo and chloro complexes of UO_2^{2+}, NpO^{2+}, Np^{4+}, and Pu^{3+} by X-ray absorption fine structure spectroscopy. *Inorg. Chem.* **36**, 4676-4683.

Ankudinov A. L., Ravel B., Rehr J. and Conradson S. D., 1998. Real-space multiple-scattering calculation and interpretation of x-ray-absorption near-edge structure. *Phys. Rev. B* **58,** 7565-7576.

Appelo C. A. J. and Parkhurst D. L. Calculating cation exchange with PHREEQC (Version 2) *http://www.hydrochemistry.eu/pub/ap_pa02.pdf*

Arai Y., Moran P. B., Honeyman B. D. and Davis J. A., 2007. In situ spectroscopic evidence for neptunium(V)-carbonate inner-sphere and outer-sphere ternary surface complexes on hematite surfaces. *Environ. Sci. Technol.* **41,** 3940-3944.

Bachmaf S., Planer-Friedrich B. and Merkel B. J., 2008. Effect of sulfate, carbonate, and phosphate on the uranium(VI) sorption behavior onto bentonite. *Radiochim. Acta* 96, 359–366.

Begg J. D., Zavarin M., Tumey S. J. and Kersting A. B., 2015. Plutonium sorption and desorption behavior on bentonite, *J. Environ. Radioact*. 141, 106–114.

Bradbury M. H. and Baeyens B., 2002. Sorption of Eu on Na- and Ca-montmorillonites: experimental investigations and modelling with cation exchange and surface complexation. *Geochim. Cosmochim. Acta* **66,** 2325-2334.

Bradbury M. H. and Baeyens B., 2006. Modelling sorption data for the actinides Am(III), Np(V) and Pa(V) on montmorillonite. *Radiochim. Acta* **94,** 619-625.

Del Nero M., Assada A., Madé B., Barillon R. and Duplâtre G., 2004. Surface charges and Np(V) sorption on amorphous Al and Fe silicates. *Chem. Geol.* 211, 15-45.

Dittrich T. M., Boukhalfa H., Ware S. D. and Reimus P. W., 2015. Laboratory investigation of the role of desorption kinetics on americium transport associated with bentonite colloids. *J. Environ. Radioact.* 148, 170–182.

Geckeis H., Schäfer T., Hauser W., Rabung Th. Missana T., Degueldre C., Möri A., Eikenberg J., Fierz Th. and Alexander W. R., 2004. Results of the colloid and radionuclide retention experiment (CRR) at the Grimsel Test Site (GTS), Switzerland – impact of reaction kinetics and speciation on radionuclide migration. *Radiochim. Acta* 92, 765–774.

García-García S., Wold S. and Jonsson M., 2007. Kinetic determination of critical coagulation concentration for sodium and calcium montmorillonite colloids in NaCl and $CaCl_2$ aqueous solutions. *J. Colloid Interface Sci*. 315, 512–519.

Gückel K., Rossberg A., Müller K., Brendler V., Bernhard G. and Foerstendorf H., 2013. Spectroscopic Identification of Binary and Ternary Surface Complexes of Np(V) on Gibbsite. *Environ. Sci. Technol.* **47,** 14418-14425.

Hellä P., Pitkänen P., Löfman J., Partamies S., Vuorinen U., Wersin P., 2014, Safety Case for the Disposal of Spent Nuclear Fuel at Olkiluoto. Posiva report 2014-04. Eurajoki: Posiva Oy.

Huber F., Kunze P., Geckeis H. and Schäfer T., 2011. Sorption reversibility kinetics in the ternary system radionuclide–bentonite colloids/nanoparticles–granite fracture filling material. *Appl. Geochem*. **26**, 2226–2237.

Hug S.J. and Sulzberger B., 1994. In-situ Fourier-transform infrared spectroscopic evidence for the formation of several different surface complexes of oxalate on TiO_2 in the aqueous-phase. *Langmuir* **10**, 3587 – 3597.

Huittinen N., Rabung T., Schnurr A., Hakanen M., Lehto J. and Geckeis H., 2012. New insight into Cm(III) interaction with kaolinite - Influence of mineral dissolution. *Geochim. Cosmochim. Acta* **99,** 100-109.

Hursthouse A. S., Baxter M. S., Livens F. R. and Duncan H. J., 1991. Transfer of Sellafield-Derived Np-237 to and within the Terrestrial Environment. *J. Environ. Radioact.* **14**, 147–174.

Hölttä P., Poteri A., Hakanen M. and Hautojärvi A., 2004. Fracture flow and radionuclide transport in block–scale laboratory experiments. **Radiochim. Acta 92**, 775–779.

Hölttä P., Siitari-Kauppi M., Leskinen A. and Poteri A., 2008. Retardation of mobile radionuclides in granitic rock fractures by matrix diffusion. *Phys. Chem. Earth*. **33**, 983–990.

Ikeda-Ohno A., Hennig C., Rossberg A., Funke H., Scheinost A. C., Bernhard G. and Yaita T., 2008. Electrochemical and complexation behavior of neptunium in aqueous perchlorate and nitrate solutions. *Inorg. Chem.* **47,** 8294-8305.

Jokelainen L., Ikonen J., Read D., Hellmuth K.-H. and Siitari-Kauppi M., 2009. The diffusion of tritiated water, chloride and uranium through granite. In: Scientific basis for nuclear waste management XXXIII, MRS Proceedings 1193, 461–468.

Jones L. H. and Penneman R. A., 1953. Infrared Spectra and Structure of Uranyl and Transuranium (V) and (VI) Ions in Aqueous Perchloric Acid Solution. *J. Chem. Phys.* **21,** 542-544.

Kaszuba J. P. and Runde W. H., 1999. The aqueous geochemistry of neptunium: dynamic control of soluble concentrations with applications to nuclear waste disposal. *Environ. Sci. Technol*. **33**, 4427–4433.

Kienzler B., Vejmelka P., Romer J., Fanghänel E., Jansson M., Eriksen T.E. and Wikberg P., 2003. Swedish-German actinide migration experiment at ÄSPÖ hard rock laboratory. *J. Contam. Hydrol.* **61**, 219–233.

Koningsberger D. C. and Prins R., 1988. X-ray absorption: principles, applications, techniques of EXAFS, SEXAFS, and XANES. John Wiley and Sons, New York, NY.

Kozai N., Yamasaki S. and Ohnuki T., 2014. Application of simplified desorption method to study on sorption of americium(III) on bentonite. *J. Radioanal. Nucl. Chem.* **299,** 1571-1579.

Kumata M. and Vandergraaf T. T., 1998. Experimental study on neptunium migration under in situ geochemical conditions. *J. Contam. Hydrol.* **35**, 31–40.

Kumpulainen S. and Kiviranta L., 2010. *Mineralogical and Chemical Characterization of Various Bentonite and Smectite-Rich Clay Materials*. Working report **2010-52**.

Kupcik T., Rabung T., Lützenkirchen, J., Finck, N., Geckeis, H. and Fanghänel, T., 2016, Macroscopic and spectroscopic investigations on Eu(III) and Cm(III) sorption onto bayerite (β-$Al(OH)_3$) and corundum (α-Al_2O_3). *J. Colloid Interface Sci.* **461,** 215-224.

Lagaly G. and Ziesmer S., 2003. Colloid chemistry of clay minerals: the coagulation of montmorillonite dispersions. *Adv. Colloid Interface Sci*. **100-102**, 105–128.

Lefèvre G., 2004. In situ Fourier-transform infrared spectroscopy studies of inorganic ions adsorption on metal oxides and hydroxides. *Adv. Colloid Interface Sci.* **107,** 109-123.

Li P., Liu Z., Ma F., Shi Q. L., Guo Z. J. and Wu W. S., 2015. Effects of pH, ionic strength and humic acid on the sorption of neptunium(V) to Na-bentonite. *J. Mol. Liq.* **206**, 285–292.

Marques Fernandes M., Baeyens B., Dähn R., Scheinost A. C. and Bradbury M. H., 2012. U(VI) sorption on montmorillonite in the absence and presence of carbonate: A macroscopic and microscopic study. *Geochim. Cosmochim. Acta* **93,** 262-277.

Marty N. C. M., Cama J., Sato T., Chino D., Villiéras F., Razafitianamaharavo A., Brendlé J., Giffaut E., Soler J. M., Gaucher E. C. and Tournassat C. 2011. Dissolution kinetics of synthetic Na-smectite. An integrated experimental approach. *Geochim. Cosmochim. Acta* **75**, 5849-5864.

Missana T., Alonso U. and Turrero M. J., 2003. Generation and stability of bentonite colloids at the bentonite/granite interface of a deep geological radioactive waste repository. *J. Contam. Hydrol.* **61**, 17–31.

Missana T., García-Gutiérrez M. and Alonso U., 2004. Kinetics and irreversibility of cesium and uranium sorption onto bentonite colloids in a deep granitic environment. *Appl. Clay Sci.* **26**, 137–150.

Missana T., Alonso U., García-Gutiérrez M. and Mingarro M., 2008. Role of bentonite colloids on europium and plutonium migration in a granite fracture, *Appl. Geochem*. **23**, 1484–1497.

Missana T., Alonso U., Albarran N., García-Gutierrez M. and Cormenzana J. l., 2011. Analysis of colloids erosion from the bentonite barrier of a high level radioactive waste repository and implications in safety assessment. *Phys. Chem. Earth.* **36**, 1607–1615.

Missana T., Benedicto A., Garcia-Gutierrez M. and Alonso U., 2014. Modeling cesium retention onto Na-, K- and Ca-smectite: Effects of ionic strength, exchange and competing cations on the determination of selectivity coefficients. *Geochim. Cosmochim. Acta* **128,** 266-277.

Müller K., Foerstendorf H., Brendler V. and Bernhard G., 2009. Sorption of Np(V) onto TiO_2, SiO_2, and ZnO: an in situ ATR FT-IR spectroscopic study. *Environ. Sci. Technol.* **43,** 7665-7670.

Müller K., Foerstendorf H., Meusel T., Brendler V.. Lefevre G., Comarmond M. J. and Payne T. E. 2012. Sorption of U(VI) at the TiO sub(2)-water interface: An in situ vibrational spectroscopic study. *Geochim. Cosmochim. Acta* **76,** 191-205.

Müller K., Gröschel A., Rossberg A., Bok F., Franzen C., Brendler V. and Foerstendorf H., 2015. In situ Spectroscopic Identification of Neptunium(V) Inner-Sphere Complexes on the Hematite-Water Interface. *Environ. Sci. Technol.* **49,** 2560-2567.

Myllykylä E., Tanhua-Tyrkkö M., Bouchet A. and Tiljander M., 2013. Dissolution experiments of Na- and Ca-montmorillonite in groundwater simulants under anaerobic conditions. *Clay Miner.* **48**, 295-308.

Möri A., Alexander W. R., Geckeis H., Hauser W., Schäfer T., Eikenberg J., Fierz Th., Dequeldre C. and Missana T., 2003. The colloid and radionuclide retardation experiment at the Grimsel Test Site: influence of bentonite colloids on radionuclide migration in a fractured rock. *Colloids Surf. A: Physicochem. Eng. Aspects* **217**, 33–47.

Nagasaki S. and Tanaka S., 2000. Sorption equilibrium and kinetics of NpO_2^+ on dispersed particles of Na-montmorillonite. *Radiochim. Acta* **88**, 705-709.

Newville M., 2004. Fundamentals of XAFS. *Consortium for Advanced Radiation Sources*, University of Chicago, Chicago, IL, version 1.7.

Park C., Kienzler B., Vejmelka P. and Jeong J., 2012. Modeling and analysis of the migration of HTO and ^{237}Np in a fractured granite core at the Äspö hard rock laboratory. *Radiochim. Acta* **100**, 197-205.

Parkhurst D. L. and Appelo C. A. J., 2013. Description of input and examples for PHREEQC version 3; a computer program for speciation, batch-reaction, one-

dimensional transport, and inverse geochemical calculations. *U. S. Geological Survey Techniques and Methods* **06-A43**.

Pastina B. and Hellä P., 2006, Expected Evolution of a Spent Nuclear Fuel Repository at Olkiluoto. Posiva-2006-5. Olkiluoto: Posiva Oy.

Pathak P. N. and Choppin G. R., 2007. Silicate complexation of NpO_2^+ ion in perchlorate media. *J. Radioanal. Nucl. Chem.* **274,** 3-7.

Poeter E. P., Hill M. C., Banta E. R., Mehl S. and Christensen S., 2006. UCODE_2005 and six other computer codes for universal sensitivity analysis, calibration, and uncertainty evaluation constructed using the JUPITER API. *U. S. Geological Survey Techniques and Methods* **06-A11**.

POSIVA OY, Loppusijoituksen perusteet [Homepage of Posiva Oy], [Online]. Available: http://www.posiva.fi/loppusijoitus/loppusijoituksen_perusteet#.U5raJJR_uoF [06/13, 2014].

Ren X., Wang S., Yang S. and Li J., 2010. Influence of contact time, pH, soil humic/fulvic acids, ionic strength and temperature on sorption of U(VI) onto MX-80 bentonite, *J. Radioanal. Nucl. Chem.* **283**, 253–259.

Sabodina M. N., Kalmykov S. N., Sapozhnikov Yu. A. and Zakharova E. V., 2006. Neptunium, plutonium and ^{137}Cs sorption by bentonite clays and their speciation in pore waters. *J. Radioanal. Nucl. Chem.* **270,** 349-355.

Schnurr A., Marsac R., Rabung T., Lützenkirchen J., and Geckeis H., 2015. Sorption of Cm(III) and Eu(III) onto clay minerals under saline conditions: Batch adsorption, laser-fluorescence spectroscopy and modeling. *Geochim. Cosmochim. Acta* **151**, 192-202.

Schäfer T., Geckeis H., Bouby M. and Fanghänel T., 2004. U, Th, Eu and colloid mobility in a granite fracture under near-natural flow conditions. *Radiochim. Acta* **92**, 731–737.

Soderholm L., Antonio M. R., Williams C. and Wasserman S. R., 1999. XANES spectroelectrochemistry: A new method for determining formal potentials. *Anal. Chem.* **71**, 4622-4628.

Soltermann D., Baeyens B., Bradbury M. H. and Marques Fernandes M., 2014. Fe(II) Uptake on Natural Montmorillonites. II. Surface Complexation Modeling. *Environ. Sci. Technol.* **48,** 8698-8705.

Tombácz E. and Szekeres M., 2004. Colloidal behavior of aqueous montmorillonite suspensions: the specific role of pH in the presence of indifferent electrolytes. *Appl. Clay Sci.* **27**, 75–94.

Turner G. D., Zachara J. M. McKinley J. P. and Smith S. C., 1996. Surface-charge properties and UO_2^{2+} adsorption of a subsurface smectite. *Geochim. Cosmochim. Acta* **60**, 3399-3414.

Turner D. R., Pabalan R. T. and Bertetti F. P., 1998. Neptunium(V) sorption on montmorillonite: An experimental and surface complexation modeling study. *Clays Clay Miner.* **46,** 256-269.

Verma P. K., Pathak P. N., Mohapatra P. K., Godbole S. V., Kadam R. M., Veligzhanin A. A., Zubavichus Y. V. and Kalmykov S. N., 2014. Influences of different environmental parameters on the sorption of trivalent metal ions on bentonite: batch sorption, fluorescence, EXAFS and EPR studies. *Environ. Sci.: Processes Impacts* **16**, 904–915.

Vieno T and Nordman H., 1999, Safety assessment of spent fuel disposal in Hästholmen, Kivetty, Olkiluoto and Romuvaara. 99-07. Helsinki: Posiva Oy.

Virtanen S., Bok F, Ikeda-Ohno A., Rossberg A., Lützenkirchen J., Rabung T., Lehto J. and Huittinen N., 2016. The specific sorption of Np(V) on the corundum (α-Al_2O_3) surface in the presence of trivalent lanthanides Eu(III) and Gd(III): A batch sorption and XAS study. *J. Colloid Interface Sci.* **483**, 334-342.

Viswanathan H. S., Robinson B. A., Valocchi A. J. and Triay I. R., 1998. A reactive transport model of neptunium migration from the potential repository at Yucca Mountain. *J. Hydrol.* **209,** 251-280.

Wang, P., Anderko, A. and Turner, D.R., 2001. Thermodynamic Modeling of the Adsorption of Radionuclides on Selected Minerals. I: Cations. *Ind. Eng. Chem. Res.* **40**, 4428–4443.

Wendt, S., 2009, Sorption and Direct Speciation of Neptunium(V) on Aluminium Oxide and Montmorillonite, Department of Chemistry, Pharmacy and Geosciences of the Johannes Gutenberg - University Mainz.

Yusov A. B., Fedoseev A. M., Isakova O. V. and Delegard C. H., 2005. Complexation of Np(V) with Silicate Ions. *Radiochemistry* **47,** 39-43.

Zavarin M., Powell B. A., Bourbin M., Zhao P. and Kersting A. B., 2012. Np(V) and Pu(V) Ion Exchange and Surface-Mediated Reduction Mechanisms on Montmorillonite. *Environ. Sci. Technol.* **46,** 2692-2698.

Zhao P., Tinnacher R. M., Zavarin M. and Kersting A. B., 2014. Analysis of trace neptunium in the vicinity of underground nuclear tests at the Nevada National Security Site. *J. Environ. Radioact.* **137**, 163–172.

Zong P., Wu X., Gou J., Lei X., Liu D. and Deng H., 2015. Immobilization and recovery of uranium(VI) using Na-bentonite from aqueous medium: equilibrium, kinetics and thermodynamics studies. *J. Mol. Liq.* **209**, 358–366.